Article

Effect of Minimum Quantity of Lubricant on Carbide Tools and Surface Integrity in the Machining of Titanium Aluminides

Enrique García-Martínez [1,2], Valentín Miguel [1,2,*] and Alberto Martínez-Martínez [2]

[1] Higher Technical School of Industrial Engineering of Albacete, University of Castilla-La Mancha, 02071 Albacete, Spain; enrique.gmartinez@uclm.es
[2] Regional Development Institute, Science and Engineering of Materials, University of Castilla-La Mancha, 02071 Albacete, Spain; alberto.martinez@uclm.es
* Correspondence: valentin.miguel@uclm.es

Abstract: Titanium aluminides are being explored as potential materials for the aeronautical sector. However, their application is limited by the high costs of processing and their difficulties in machining. This research evaluates the effectiveness of the minimum quantity lubrication technique (MQL) on the turning process of Ti48Al2Cr2Nb aluminide in terms of tool wear, tool life, cutting forces, surface integrity, and temperature. It was found that MQL conditions can improve the process efficiency, reducing the thermally induced wear mechanisms and enlarging the tool life compared to dry machining. Furthermore, it allows the cutting speed to be incremented, leading to lower processing times. However, MQL seems to not be effective in the reduction of the strain-hardening effect near the machined surface and, although the number of microcracks is reduced, defect-free surfaces cannot be obtained. Moreover, similar microstructural alterations as for dry cutting were detected. The best cutting conditions in terms of surface quality were assessed using the central composite face (CCF) design and surface response methodology. Optimization of the surface roughness under industrially viable cutting conditions was achieved with an average surface roughness value, Ra, of 0.29 μm (feed rate of 0.05 mm/rev, a cutting speed of 54.6 m/min and a depth of cut of 0.125 mm).

Keywords: MQL; titanium aluminides; machining; surface integrity

1. Introduction

Titanium and titanium alloys are considered key materials for aerospace and automotive applications due to their attractive properties, such as low density, good corrosion resistance, and high strength-to-weight ratio. Traditionally, Ti6Al4V has been extensively implemented in aeronautical parts, being about 50% of all titanium alloys used [1]. Nevertheless, this alloy is not able to be used in hot parts of aero engines (combustors and turbines) because temperatures in these zones can reach higher than 600 °C. For these applications, nickel-based superalloys are currently preferred, thanks to their excellent resistance to high-temperature conditions [2].

In recent decades, intermetallic titanium aluminides have gained interest as possible substitutes for nickel-based superalloys in high-temperature applications due to their offering a combination of appropriate features. These alloys show high specific modulus and specific strength for temperatures higher than 600 °C and good oxidation resistance. In comparison to Ti6Al4V, whose creep limit is about 385 °C, titanium aluminides exhibit a creep limit higher than 1000 °C [3,4]. Moreover, titanium aluminide density is about 4 g/cm^3, about half that of superalloys, which results in a weight reduction, leading to important fuel consumption savings. In contrast, titanium aluminides exhibit low ductility (<2%) and fracture toughness at room and low temperatures [5].

Among the different aluminides, γ titanium aluminides (TiAl alloys), whose aluminum content ranges between 46 and 66% are usually preferred [6]. In particular, Ti48Al2Cr2Nb alloy stands out, showing increased ductility at lower temperatures compared to other TiAl alloys, despite its inherent brittle behavior, thanks to the addition of chromium. Some specific parts of aero-engines have already been successfully manufactured and implemented with this alloy [7]. Nevertheless, because of the absence of processing methods suitable for materials with limited ductility, the applicability of TiAl alloys is restricted [8]. Manufacturing processes such as casting [9], powder metallurgy, ingot metallurgy, vacuum arc remelting (VAR), and, thanks to the recent advance of additive manufacturing [10,11], electron beam melting (EBM) [12], are applicable. The major disadvantage of these manufacturing procedures is that the part surface quality and the geometrical precision achieved do not fulfill the challenging specifications of the aeronautical sector [13]. Hence, it is imperative to undergo some finishing machining processes to fulfill the necessary criteria.

Nevertheless, TiAl alloys are reported as hard-to-cut materials, exhibiting extremely low machinability that leads to rapid tool wear, high cutting forces, and consequently, some damage to the machined parts' surface quality. Their low thermal diffusivity favors the temperature increment in the cutting area, and the chemical affinity and friction coefficient with cutting tools material promote adhesive and abrasive wear phenomena, leading to a reduced tool life [14]. Moreover, the brittle behavior of TiAl alloys affects chip formation, resulting in a short tool-chip contact area that encourages the plastic deformation of the cutting edge and promotes the surface microcracking of the machined part.

Although some research can be found in the literature regarding the experimental and analytical evaluation of traditional machining processes such as turning [15], drilling [16], and milling [17] on titanium aluminides, the number of studies is quite low in comparison to other titanium alloys, so further efforts are needed to find the best cutting conditions. Most of the studies completed on turning conclude the need to perform the process with low cutting speeds, avoiding thermal increase and rapid deterioration of the tool [18]. This sometimes leads to non-productive times for the industry with low efficiencies. Although most authors have focused on evaluating the performance of carbide tools, some attempts have been made with PCD tools, reporting a slight increase in tool life, which, together with the high cost of these inserts, is still far from being a viable option [19]. In a recent study, it has been shown that geometrical optimization of the tool by increasing the clearance angle to decrease the frictional effects on the tool flank allows the cutting speed to be increased by 50% while controlling tool wear [20].

In terms of part surface integrity, microcracking has been reported as the most important issue. Beranoagirre et al. [21] reported that the limitation of superficial cracks induced by machining is crucial for the performance of titanium aluminide parts since they can cause catastrophic failure of the material. In this aspect, Yao et al. [22] concluded that the feed rate and the depth of cut strongly influence the surface quality; meanwhile, the cutting speed does not show a remarkable effect, due to the brittleness of TiAl alloys. Recently, Wang and Liu [18] established that reducing the feed rate and the depth of cut helps improve the surface quality. Only some authors have reported crack-free surfaces, favored by thermal-softening derived from high-speed machining [23]. Nevertheless, uncontrollable tool wear takes place which renders the process inoperative.

Residual stress generation and the hardening tendency of titanium aluminides during machining operations, because of the high cutting forces and high friction coefficient, have also been evaluated [22]. In contrast to most metals, the predominant force is the radial component, known as the repulsion force, which is proof of low machinability [14]. The hardening effect on the machined subsurface is due to the plastic lamellar deformation and the ability of TiAl alloys to maintain mechanical strength at high temperatures [24]. Hardened layer depths of 300 μm have been observed with compressive stresses higher than 500 MPa. The increment of the flank wear promotes the mechanical and thermal loads to be increased, leading to higher residual stresses [25]. However, the

occurrence of compressive stresses can be taken as advantageous in the case of fatigue-stressed parts.

To control tool wear and avoid superficial damage to the workpiece, different lubrication strategies have been employed. Traditional flood lubrication has not been reported as effective in tool wear control, since severe thermal shocks could accelerate tool wear. Priarone et al. [26] found reduced tool life when applied to wet machining compared to dry conditions. Moreover, the environmental implications arising from the substantial amount of pollutants generated emphasize the necessity of addressing coolants and lubricants as mandatory topics [27].

The minimum quantity of lubrication technique, consisting of applying a small quantity of lubricant, in the form of atomized droplets, mixed with air has been identified as an environmentally sustainable solution [28]. Some efforts have been developed in titanium aluminide machining. Priarone et al. [29] highlighted MQL efficiency for the milling process but found it ineffective for turning, due to the lack of cooling effect. Klocke et al. [30] established that similar results were obtained under MQL and flood conventional lubrication. However, none of these investigations was performed with an optimized tool geometry. Only the combination of high-speed machining strategy and MQL condition was conducted to crack-free surfaces. Despite this, there was deformation of subsurface lamellae. Nevertheless, as mentioned above, excessive tool wear took place. In the same research, Klocke et al. [30] compared MQL and cryogenic lubrication techniques, although the efficiency of the last one in titanium alloy machining processes is unclear, with contradictory results for tool life.

In previous research [31], the application of MQL and cryogenic lubrication techniques on TiAl alloys was evaluated in terms of economics and industrial sustainability. MQL was reported as the more sustainable technique, thanks to the lower impact on the carbon footprint, while cryogenic lubrication leads to excessive LN2 consumption which generates a high environmental impact. For this reason, and given the lack of studies on the optimization of the MQL technique on titanium aluminides, more research effort is needed on this topic, especially on the fundamental aspects of tool wear and surface integrity of the machined parts. In this sense, this research aims to analyze the influence of MQL lubrication on the turning process of Ti48Al2Cr2Nb aluminide for the optimum cutting conditions found in previous research. The effectiveness is analyzed in terms of tool life, cutting forces, surface quality, microstructural alterations, and subsurface hardening, comparing the results with dry cutting. Furthermore, the performance of using biodegradable olive oil is analyzed, ensuring environmentally sustainable conditions.

2. Materials and Methods

Tests were conducted on Ti48Al2Cr2Nb alloy via turning processes. The chemical composition is detailed in Table 1. The workpieces, 57 mm diameter rods, were initially manufactured using a vacuum arc furnace and then subjected to hot isostatic pressing (HIP) to improve microstructure uniformity and reduce porosity defects.

Table 1. Ti48Al2Cr2Nb chemical composition (wt%).

Ti	Al	Nb	Cr	C	H	N	O
59.10	33.45	4.72	2.51	0.005	0.001	0.007	0.045

The cylinders were machined on a semi-automatic lathe Microcut H-2160 (Buffalo Machinery Co., Ltd., Taichung, Taiwan) equipped with a variable frequency drive to select the cutting speed level required for each trial. TNMG 160408-SM H13A uncoated carbide tool with a radius, r_e, of 0.8 mm was selected. According to previous research [20], MTJNR 2525M 16M1 tool holder from Sandvik Coromant (Sandvik Corp., Stockholm, Sweden). A custom-made shim was utilized to set the back rake angle precisely, leading to $\gamma_y = 0°$,

and a back clearance angle $\alpha_y = 15°$, through which the optimal cutting parameters were identified.

To assess the effectiveness of both lubrication conditions, dry and MQL long-distance experiments were conducted, maintaining a constant feed rate (f = 0.1 mm/rev) and depth of cut ($a_P = 0.25$ mm) while adjusting the cutting speed within the range of 50 m/min to 70 m/min. Although the ratio a_P/r_e is lower than that recommended by the manufacturer (2/3), $a_P = 0.25$mm is the maximum one for the machine under reasonable conditions. In the case of MQL conditions, refined olive oil was opted for due to its high biodegradability and wide availability. Utilizing a Steidle Lubrimat L60 device (Steidle GmbH, Leverkusen, Germany), the cutting oil was atomized directly onto the rake face, as depicted in Figure 1. A flow rate of 25 ml/h was maintained, accompanied by an air pressure of 4 bar, representing an intermediate value within the maximum possible flow rate range of the instrument. Tests persisted until the tool breakage, which was determined by a flank wear criterion of $V_b = 0.100$ mm. The evaluation of flank wear occurred every 200-250 m of cutting length using an Olympus SZX7 stereomicroscope. The three components of the cutting force were continuously registered by using a three-axes dynamometer equipped with four strain-gages load cells, manufactured by the research team and validated for previous research [32]. The tool-workpiece contact temperature was evaluated by applying the natural tool-workpiece thermocouple technique. This technique consists of using the workpiece and the tool as the pair constituting the hot extreme of the thermocouple. By using a thermometer unit, the thermocouple effect between the hot and the cold extremes was registered. In this way, the cutting area was the hot joint; meanwhile, the areas far from that zone, tool holder and tool machine, constitute the cold extreme. This technique requires a specific calibration methodology. More details about the use of this procedure for Ti48Al2Cr2Nb-WC/Co pair can be found in specific research [33].
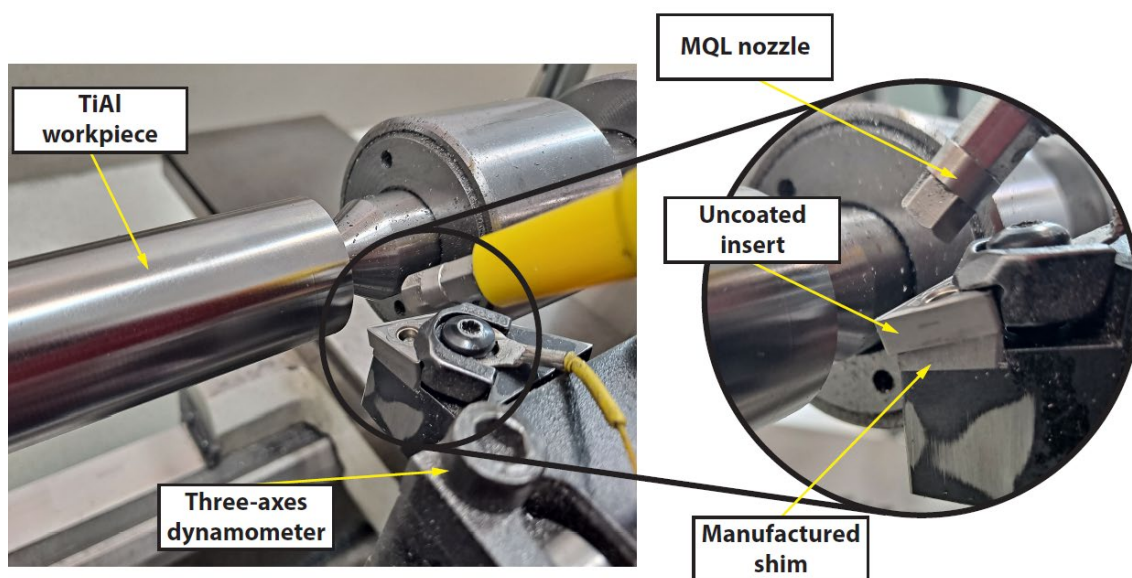

Figure 1. Detail of the MQL nozzle placement.

The cutting speed's influence on surface integrity, subsurface hardening, and microstructural alterations was analyzed under MQL conditions. The analysis was performed at the beginning of the machining (within the first 10–20 cm) when the tool can be considered new. The surface quality was observed by using a scanning electron microscope (SEM). To assess the subsurface alterations, the cylinders were transversally cut using wire-EDM to avoid overheating. The samples were first sanded, later polished, and finally etched for 5–10 s with a solution of 1 mL of HF, 1 mL of HNO_3, and 1 mL of acetic acid in 100 mL of solution volume. Knoop microhardness tests with a load of 50 g were carried out every 10 μm from the machined surface up to a distance of 300 μm.

Afterward, a series of short tests, up to 15 mm of feed length, were performed for the MQL condition to map the effect of the cutting variables (cutting speed, feed rate, and depth of cut) on the surface roughness, looking for the optimal conditions in terms of average surface roughness, Ra. The surface roughness was analyzed by using a roughness profilometer FormTalysurf50 (Taylor Hobson Inc., Leicester, UK) and processed using the specific Talymap Gold 6.1 software. Three random trajectories of 4 mm long were measured, reducing the influence of local individual defects. The roughness profile was separated from the wavelet profile using a 0.8 mm Gaussian filter. A central composite face (CCF), with three factors at two levels of design, was used for the optimization trials. A total number of 18 randomized runs (14 runs in the design and 4 center points), were carried out. Table 2 summarizes the input factor and their corresponding levels used in the design of experiments. For these cases, the tool wear was evaluated after each trial to ensure that no significant flank wear was modifying the cutting results. The cutting edge was changed every 3 trials.

Table 2. Cutting conditions for short-turning tests under MQL condition.

Test	Cutting Speed (m/min)	Feed Rate (mm/rev)	Depth of Cut (mm)
1	70	0.05	0.375
2	60	0.10	0.250
3	70	0.15	0.375
4	70	0.10	0.250
5	60	0.10	0.250
6	50	0.05	0.375
7	60	0.05	0.250
8	50	0.05	0.125
9	70	0.05	0.125
10	70	0.15	0.125
11	60	0.10	0.125
12	50	0.15	0.375
13	60	0.15	0.250
14	60	0.10	0.250
15	50	0.10	0.250
16	60	0.10	0.375
17	50	0.15	0.125
18	60	0.10	0.250

3. Results and Discussion

3.1. Tool Wear and Tool Life

Figure 2 shows the tool wear evolution under dry and MQL conditions for each cutting speed evaluated. As noted in previous studies, variations in cutting speed play a crucial role in the progression of flank wear, primarily driven by the elevation of cutting temperature. This leads to an accelerated wear phenomenon, as evidenced by the final increase in the wear rate in the wear curves. Comparing both lubrication conditions, MQL is effective in the reduction in the wear rate, leading to an increment of the tool life for all cutting speeds, as shown in Figure 2b. The wear rate is reduced for all cases. This phenomenon can be attributed to the lubricating properties of the olive oil. The oil droplets effectively reach the cutting zone, creating a lubricating film at the interface between the workpiece flank and the tool, as well as at the chip-tool interface. Furthermore, the inherent brittleness of the alloy results in chip fracturing without deformation, facilitating easy removal from the cutting zone and enhancing the ability of the oil to reach the contact area, thereby increasing its lubricating effectiveness. Figure 3 shows the tool wear morphology at the end of the tool life for a cutting speed of 50 m/min. As reported in previous

research [20], the primary wear mechanisms observed are adhesive and abrasive wear. Adhesion of the titanium aluminide onto the flank face of the tool is prominently visible, accompanied by the formation of a built-up layer (BUL) covering a portion of the rake face. In comparison, the BUL appears thinner in the case of Minimum Quantity Lubrication (MQL) compared to dry machining. However, the main effect benefit of MQL is seen in the rake face of the tool. The oil film helps reduce the friction in the chip–tool interface, reducing the sliding zone in the fake face. It also limits abrasive effects.
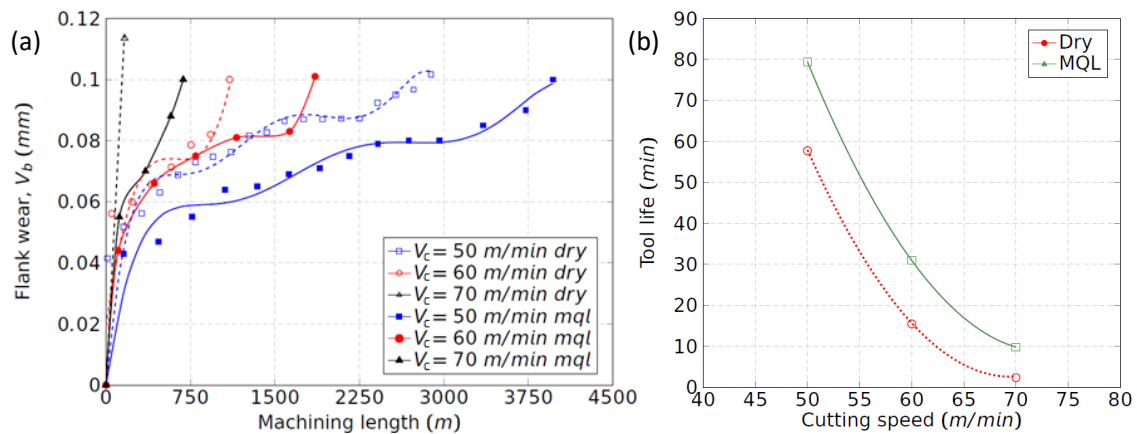
Figure 2. Tool performance under different cutting conditions: (**a**) tool wear evolution; (**b**) tool life for a maximum V_b = 0.100 mm (f = 0.1 mm/rev and a_P = 0.25 mm).
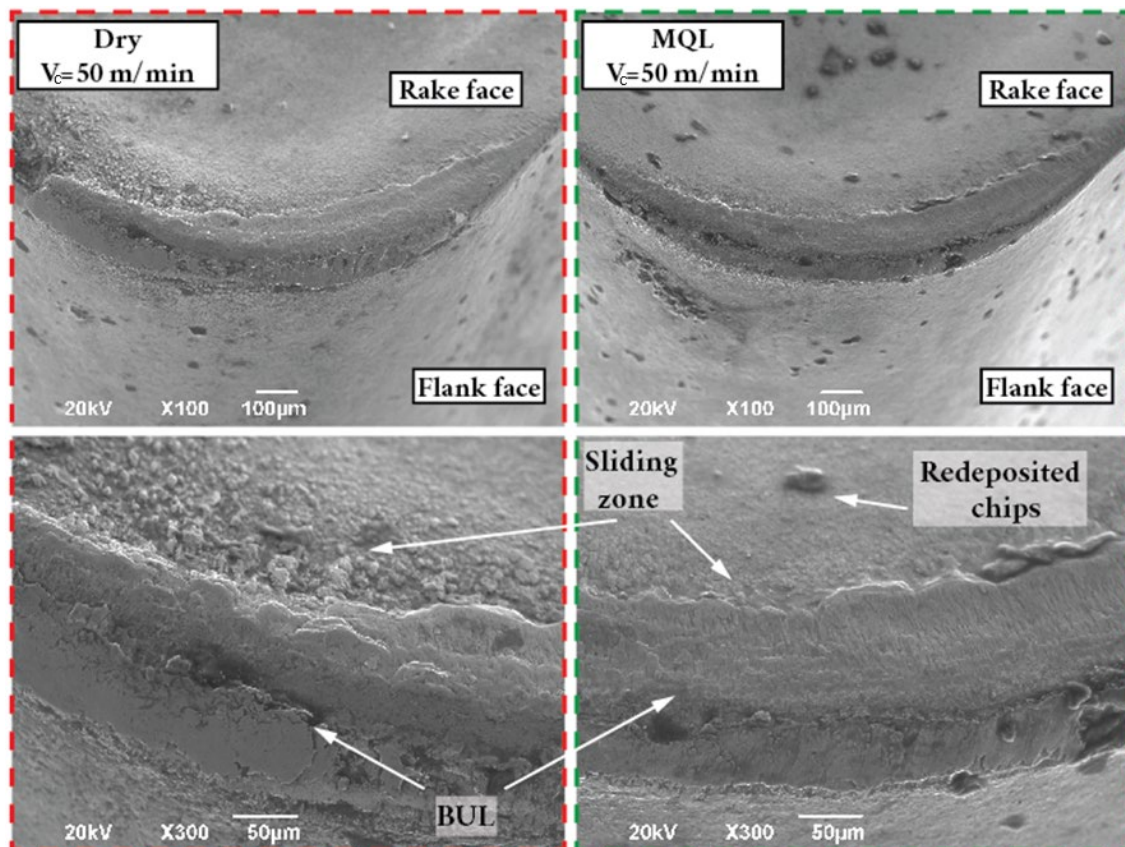

Figure 3. Tool wear morphology at the end of the tool life for V_c = 50 m/min case under MQL and dry conditions (f = 0.1 mm/rev and a_P = 0.25 mm).

According to Figure 2b, the impact of the Minimum Quantity Lubrication (MQL) condition becomes increasingly significant as the cutting speed increases. At 50 m/min, 60

m/min, and 70 m/min, the tool life is extended by 1.3, 2, and 4.1 times, respectively, compared to dry cutting. This indicates the potential of MQL for higher cutting speeds, resulting in reduced machining times when employing the MQL technique. A similar trend was found by Priarone et al. [34]. In comparison, they achieved a tool life of around 40 minutes when machining the same alloy at a cutting speed of 50 m/min, feed rate of 0.1 mm/rev, and depth of cut of 0.3 mm (a_P =0.25 mm in this study). However, this decreased to less than 10 minutes when the cutting speed was increased to 60 m/min. They utilized a flow rate of 115 ml/min of an emulsion mist (5% oil in water). Worse results were found if oil was used. This means that the combination of effective lubrication with optimized tool configuration can double the tool life, even if the cooling capacity of the oil is lower than that of the emulsion mist.

3.2. Temperature

Although the MQL technique is not focused directly on temperature reduction, it was found that the reduction in friction allows the cutting temperature to be reduced by about 100 °C. Due to the difficulty of measuring the cutting temperature because of the high values existing, which is in the upper limit of the thermocouple working range, it was decided to evaluate and compare the temperature when the cutting is interrupted. Figure 4 shows the tool-workpiece temperature due to the friction and ploughing phenomena on the flank face of the tool once the feed rate is removed, maintaining the tool in contact while the cylinder is rotating, according to the methodology established in previous research [33]. The heat is only generated in the third deformation zone (flank wear band), so the lower values found for the MQL condition imply a reduction in the friction phenomenon in that zone thanks to the effective lubrication. According to the natural thermocouple principle [33], the tool and workpiece must be in contact, closing the electrical circuit and registering the electromotive force as a function of the difference between the hot and cold junctions. If the thermocouple can measure the contact temperature, it means that the oil lubrication film is not continuous in the flank wear band, since oil is not electrically conductive. This result suggests that a discontinuous film is deposited, removed, and redeposited again with each pulse of the microlubrication system.

Furthermore, the temperature increment during the test is so much lower for MQL conditions than for dry cutting. This result is consistent with the lower wear rate obtained under MQL conditions. Probably, the final wear of the insert is mostly due to mechanical loads, affected by cutting forces and machining length, rather than thermal effects due to temperature, contrary to dry machining. Comparatively, dry turning at 70 m/min is not possible, since the cutting temperature is always higher than 900 °C. For MQL conditions, that temperature is never reached.
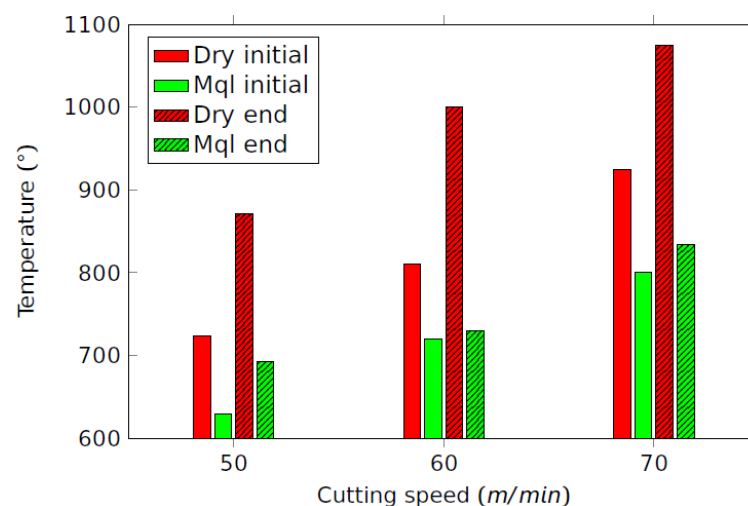

Figure 4. Tool-workpiece temperature due to friction at the beginning and the end of the trials (f = 0.1 mm/rev and a_P = 0.25 mm).

3.3. Cutting Forces

Figure 5 shows the cutting force evolution for each cutting speed under dry and MQL machining. The highest forces are the tangential and radial components, with the axial component being much lower. The high magnitude of the radial force, comparable to the tangential component, is due to the machining occurring only at a small area on the nose radius because of the lower depth of cut used in the experiments, so the chip area/tool-workpiece contact length relationship is low [35].

It is observed that the lubrication condition does not have an influence on the initial cutting forces at the beginning of the machining operation when the insert is new. This means that the specific cutting energy required to remove the chip does not change with the lubrication. Only some differences are found for the axial components, being lower for MQL cases. Nevertheless, the low values of this component are within the limit of the measuring device range, which means that the small differences may be due to the measurement process.

Comparing both lubrication conditions, the increment of the three components is lower under MQL conditions than for dry cutting. This result is more remarkable comparing the radial component, which is more influenced by the evolution of the flank wear. This is consistent with the linear relationship between the flank wear and the cutting forces reported by other authors [36]. Since the tool wear progression is lower thanks to the effective lubrication, the increment of the cutting forces is reduced. Furthermore, lower cutting force values obtained for similar flank wear conditions indicate that the normal stress in the tool-workpiece contact interface is lower under MQL conditions. This also has a beneficial reciprocal effect in reducing wear.
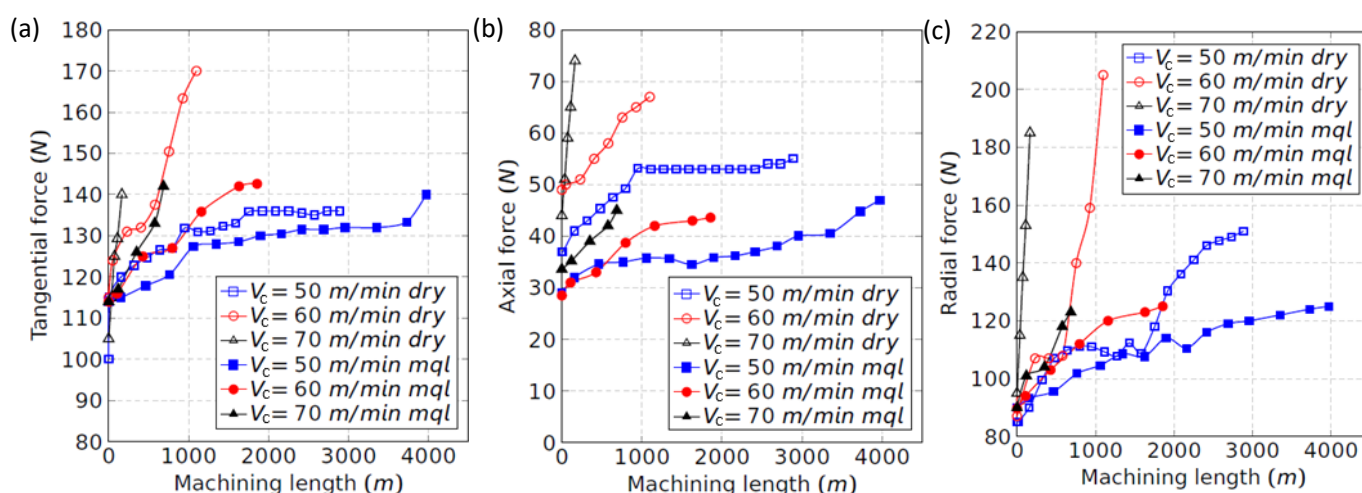

Figure 5. Cutting forces evolution under MQL and dry conditions (f = 0.1 mm/rev and a$_P$ = 0.25 mm): (**a**) tangential force; (**b**) axial force; and (**c**) radial force.

3.4. Subsurface Microhardness, Microstructural Alterations and Surface Integrity

Figure 6 shows the microhardness profile of the machined parts up to 300 µm from the machined surface under MQL conditions. The oscillations observed are due to the sensibility of the measuring method, and according to the experimental procedure and the equipment used the error is considered to have an upper limit of about 17%. Nevertheless, the hardness trends observed are clear and the oscillations are meaningless. A hardening effect is induced by the machining operation, reaching values up to double the bulk value near the machined surface. This effect is reduced as the distance from the surface increases. Similar results were obtained by other authors for different machining processes of titanium aluminides [37]. This effect is due to the lamellar deformation along the cutting speed direction near the surface, as shown in Figure 7. The capacity of strain

hardening of titanium aluminides at high temperatures has been reported in the literature. However, it causes a lack of ductility in the subsurface proximities.
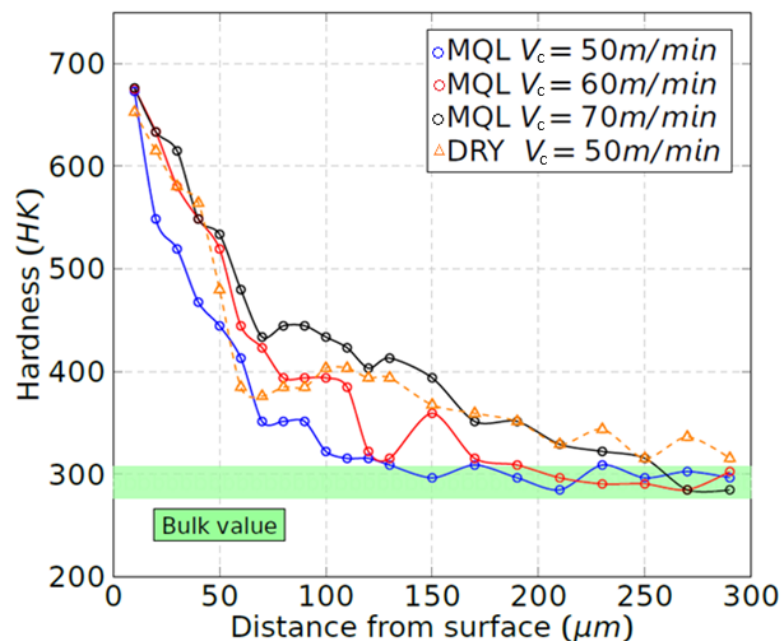

Figure 6. Knoop microhardness profile induced by the machining operations (f = 0.1 mm/rev and a$_P$ = 0.25 mm).

It was found that the cutting speed does not have a remarkable influence on the hardening effect, reaching the same maximum value for all cutting speeds experimented. Probably, the plastic limit capacity of the alloy is consumed for all conditions. The effect of the speed increment is only noticeable in a slight hardness increase at 50 μm–100 μm from the machined surface. Nevertheless, the same tendency is found in the first 50 μm, where the most important variations take place.

Compared to previous results obtained in other research focused on dry turning, similar microhardness profiles indicate that lubrication has a low influence in this aspect, as lamellar deformation occurs locally near the surface, reaching the same hardness values.

As observed in Figure 7, no noticeable differences in the subsurface microstructure alterations are found with the cutting speed, which is consistent with the microhardness profiles. The duplex microstructure consisting of γ-equiaxial grains and lamellar grains of the phases γ and α$_2$ can be seen, being the last ones responsible for the lamellar deformation. Similar microstructure alterations were observed under dry machining [20].

Regarding surface integrity, the workpieces seem to be relatively undamaged. However, some microcracks are observed, as depicted in Figure 8, which is due to the brittle behavior of this alloy. The microcracks are oriented transversely to the feed marks. This indicates that the surface breakage is produced perpendicular to the direction of the cutting speed due to the excessive lamellar deformation generated. Although these defects are found for both lubrication environments, MQL reduces the density of microcracks in comparison to dry machining, as can be observed in Figure 8 The density of defects at 50 m/min is 143 defects/mm^2 for dry machining and 87 defects/mm^2 for MQL. The reduction in friction and the normal stress in the tool-workpiece contact benefit the lower number of defects. Furthermore, increasing the cutting speed decreases the occurrence of defects, mostly when a cutting speed of 70 m/min is used and the surface appears visibly smoother, finding only 37 defects/mm^2 (57 defects/mm^2 at 60 m/min).

Nevertheless, the MQL technique does not permit obtaining totally defect-free surfaces, which can be a key factor for parts that will operate under fatigue conditions because microcracks can be a potential point for failure initiation.
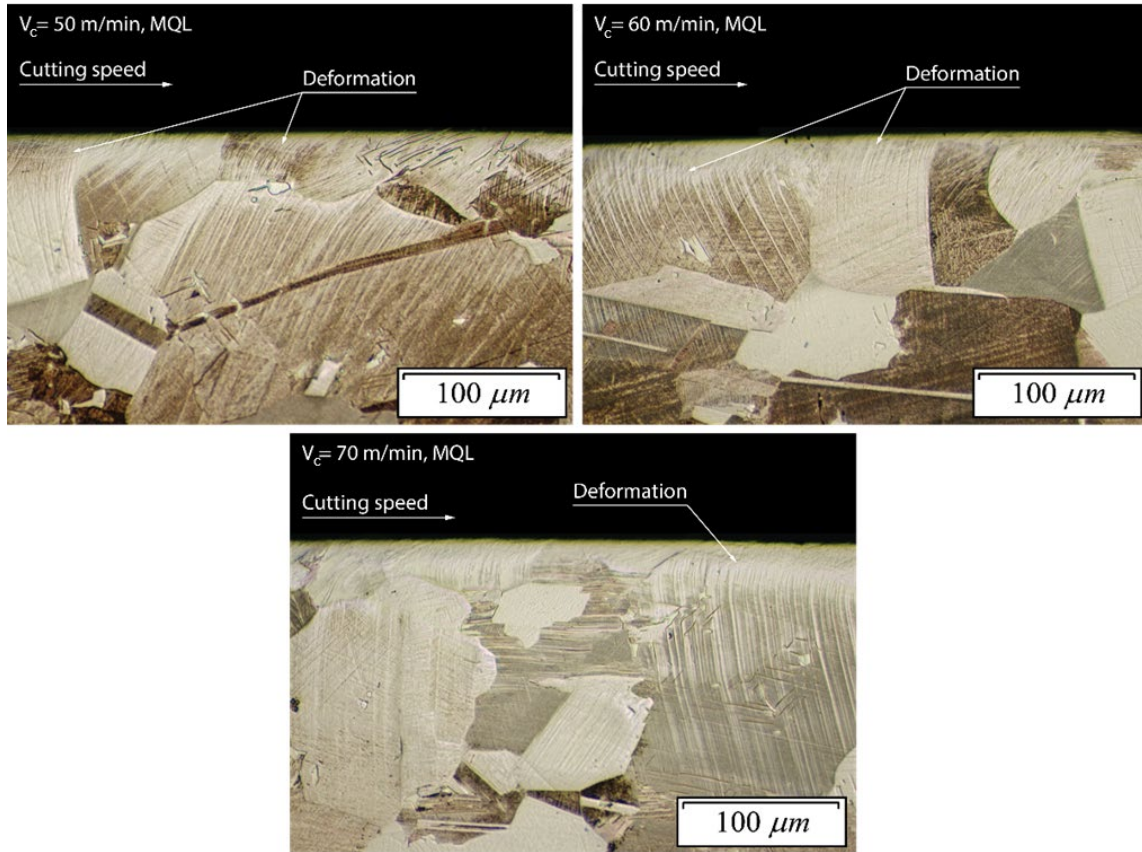

Figure 7. Subsurface microstructural alterations of the sample machined under MQL condition (f = 0.1 mm/rev and a_P = 0.25 mm).
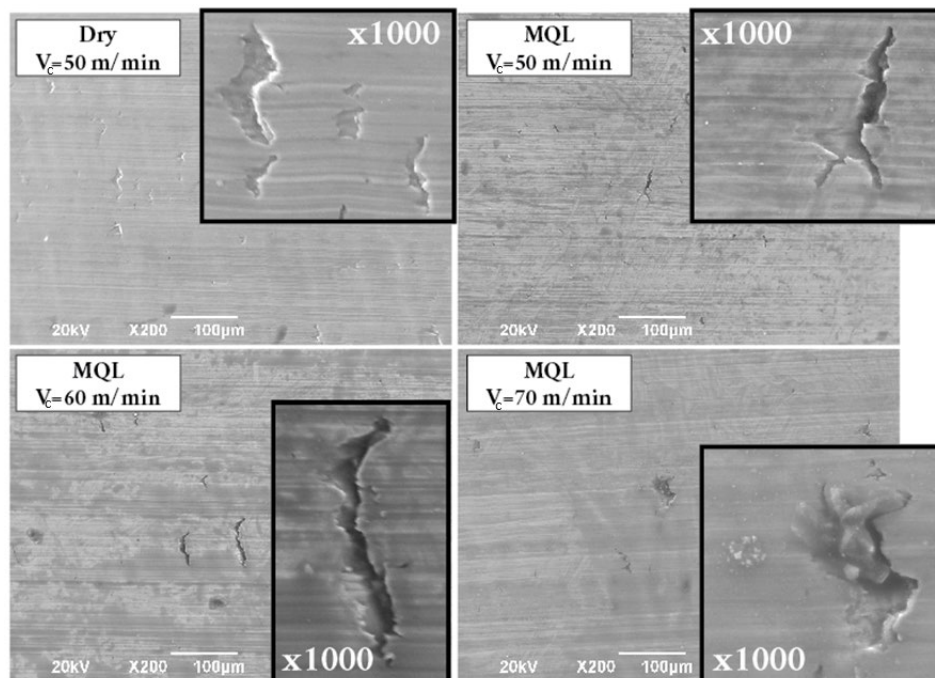

Figure 8. Surface morphology of the machined workpieces (f = 0.1 mm/rev and a_P = 0.25 mm).

3.5. Surface Roughness Statistical Analysis

According to the central composite face design developed, a surface response methodology has been applied, fitting the quadratic model to the experimental data, Equation 1. The good correlation between the experimental values and the fitted model is described by $R^2 = 0.89$. The 4D contour plots of average surface roughness, Ra, are shown in Figure 9.

$$Ra = 0.94 - 0.066V_c + 13.89f + 6.75a_p + 0.000671V_c^2 - 30.0f^2 - 7.66a_p^2 - 0.024V_c \cdot f - 0.0466V_c \cdot a_p + 1.95f \cdot d \qquad (1)$$

The surface roughness is most strongly affected by the feed rate, followed by the depth of cut. As observed in Figure 9, the increment of the feed rate from 0.05 mm/rev to 0.10 mm/rev and 0.15 mm/rev, increases the surface roughness levels (clearly see the different color levels). This result is expected according to the cutting mechanics and the cutting theory. In Figure 10a, the effect of the feed rate and the cutting speed on surface roughness for a depth of cut of 0.25 mm can be observed. Ra values lower than 0.5 µm can be obtained for the lower feed rate. However, the Ra values are doubled for 0.1 mm/rev and are tripled for 0.15 mm/rev. On the other hand, the cutting speed has a low influence on Ra, as shown in Figure 10b. Variations lower than 0.1 µm are found in the range between 50 m/min and 70 m/min. Other authors have reported the low influence of cutting speed when machining titanium aluminides due to the brittle behavior of these alloys [22]. Nevertheless, a beneficial effect is found when the cutting speed rises from 50 m/min to 60 m/min, reducing the Ra values, being the most appropriate range in terms of surface roughness, independently of the depth of cut and feed rate employed. Anwar et al. [35] reported that the increment of the cutting speed, leading to cutting temperature increases, results in enhanced plasticity and reduced brittleness of the TiAl alloy, improving the surface roughness. However, a further increase in the cutting speed leads to excessive temperatures with an adverse effect on the surface quality. For that reason, cutting speeds higher than 60 m/min always led to surface worsening.
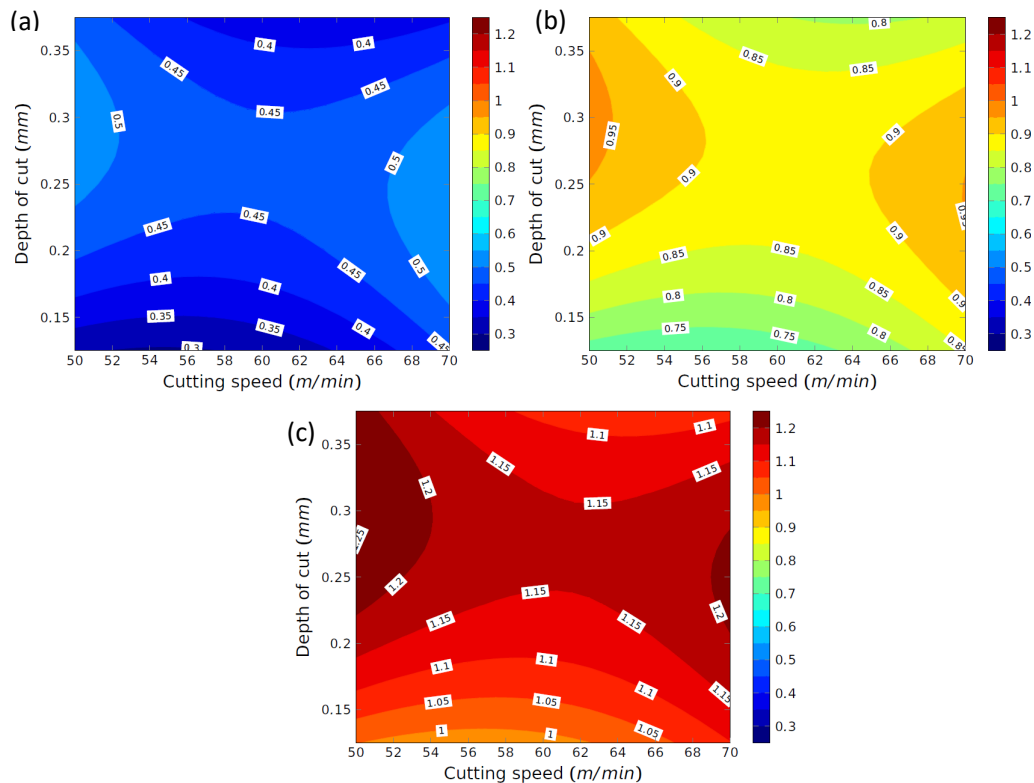

Figure 9. Four-dimensional V-d response contour plots: (**a**) f = 0.05 mm/rev; (**b**) f = 0.10 mm/rev; and (**c**) f = 0.15 mm/rev.

According to the 4D contour plots of Figure 9, the lower Ra values are found for specific combinations of depth of cut and cutting speed. Nevertheless, the same tendency is found for each feed rate level. First, the increment of the depth of cut from 0.125 mm to 0.25 mm leads to higher Ra values, independently of the other two variables analyzed. Secondly, increasing the depth of the cut up to 0.375 mm favors the reduction in the surface roughness.

The lowest Ra value is 0.29 μm, obtained for the lowest feed rate of 0.05 mm/rev, cutting speed of 54.6 m/min, and depth of cut of 0.125 mm. Furthermore, for this feed rate, the 18% cutting speed-depth of cut combinations leads to Ra values lower than 0.4 μm, the tolerance limit imposed by the rigorous demands of the aerospace sector [37].
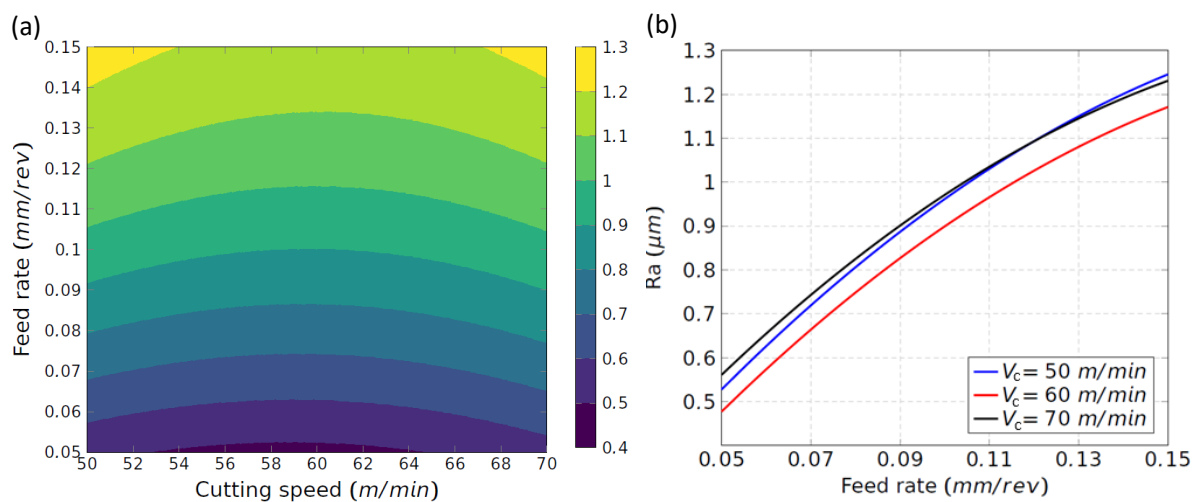

Figure 10. Roughness results in MQL tests: (**a**) 4D V-f response contour plot for $a_P = 0.25$ mm; (**b**) Ra against feed rate for $a_P = 0.25$ mm.

4. Conclusions

In this research, the effectiveness of the minimum quantity of lubricant technique was evaluated for the turning operation of Ti48Al2Cr2Nb aluminide. It was compared with dry machining in terms of tool wear, tool life, cutting forces, and temperature. Furthermore, the effect of the cutting parameters on the surface quality was analyzed by means of surface response methodology, mapping the average surface roughness, Ra, as a mean surface quality indicator. The following are summarized as more detailed results:

1. MQL has been recognized as an effective technique for reducing tool wear, attributed to the lubricating effect of oil in the cutting area. As a result, the tool life is incremented, up to 80 minutes when a cutting speed of 50 m/min is selected. Furthermore, MQL conditions make it possible to perform the process at 70 m/min, for which the tool life is four times higher than for dry cutting.

2. The discontinuous oil film deposited in the tool-workpiece interface shows a beneficial effect in temperature reduction for all cutting speeds experimented on. As a consequence, the thermally induced wear mechanisms are limited, reducing the wear rate. The adhesive wear on the flank face of the tool is reduced and the abrasion phenomenon on the rake face is limited.

3. The initial cutting forces take similar values under dry and MQL conditions. Nevertheless, their evolution with the increment of the flank wear is lower for MQL than for dry machining, which suggests that the contact normal stress in the tool-workpiece interface is reduced.

4. A strain hardening effect was detected near the machined surface, induced by the lamellar deformation along the cutting speed direction. Values up to double the bulk hardness are reached for all cutting speed values. However, MQL is not effective in this respect.

5. Some microcracking was found for both lubrication conditions. Nevertheless, MQL has been reported to be effective in reducing the number of surface defects. Increasing the cutting speed also decreases the number of microcracks.

6. The statistical analysis for the surface quality of the machined parts under MQL conditions shows that the feed rate is the most influential variable, being that the effect of cutting speed is very low. The effective combination of depth of cut and cutting speed allows Ra values below 0.4 μm to be obtained. The optimum Ra was set at 0.29 μm, for a feed rate of 0.05 mm/rev, a cutting speed of 54.6 m/min, and a depth of cut of 0.125 mm.

Author Contributions: Conceptualization, V.M.; methodology, E.G.-M. and A.M.-M.; validation, V.M., E.G.-M. and A.M.-M.; formal analysis, V.M. and E.G.-M.; investigation, E.G.-M. and A.M.-M.; resources, V.M.; data curation, E.G.-M. and A.M.-M.; writing—original draft preparation, E.G.-M. and V.M.; writing—review and editing, V.M. and E.G.-M.; visualization, V.M., E.G.-M. and A.M.-M.; supervision, V.M.; project administration, V.M.; funding acquisition, V.M. All authors have read and agreed to the published version of the manuscript.

Data Availability Statement: "The raw data supporting the conclusions of this article will be made available by the authors on request."

Conflicts of Interest: The authors declare no conflicts of interest.

References

1. Leyens, C.; Peters, M. (Eds.) *Titanium and Titanium Alloys*; Wiley: Hoboken, NJ, USA, 2003; ISBN 9783527305346.
2. Prashar, G.; Thakur, K.; Singh, S.; Singh, P.; Srivastava, V.K. Superalloys for high-temperature applications: An overview. In Proceedings of the AIP Conference Proceedings, Phagwara, India, 29–30 July 2022; p. 020022.
3. Appel, F.; Wagner, R.; Kumar, V. Intermetallics: Titanium Aluminides. In *Reference Module in Materials Science and Materials Engineering*; Elsevier: Amsterdam, The Netherlands, 2017.
4. Mouritz, A.P. Titanium alloys for aerospace structures and engines. In *Introduction to Aerospace Materials*; Elsevier: Amsterdam, The Netherlands; Woodhead Publishing Limited: Cambridge, UK, 2012; pp. 202–223.
5. Castellanos, S.; Cavaleiro, A.; Jesus, A. de; Neto, R.; Alves, J.L. Machinability of titanium aluminides: A review. *Proc. Inst. Mech. Eng. Part L J. Mater. Des. Appl.* **2018**, *233*, 146442071880938. https://doi.org/10.1177/1464420718809386.
6. Boyer, R.; Welsch, G.; Colllings, E.W. *Materials Properties Handbook: Titanium Alloys*; ASM International, Ed.; ASM International: Almere, the Netherlands, 1993; ISBN 9780871704818.
7. Bewlay, B.P.; Nag, S.; Suzuki, A.; Weimer, M.J. TiAl alloys in commercial aircraft engines. *Mater. High Temp.* **2016**, *33*, 549–559. https://doi.org/10.1080/09603409.2016.1183068.
8. Kothari, K.; Radhakrishnan, R.; Wereley, N.M. Advances in gamma titanium aluminides and their manufacturing techniques. *Prog. Aerosp. Sci.* **2012**, *55*, 1–16. https://doi.org/10.1016/j.paerosci.2012.04.001.
9. Yu, W.; Zhou, J.; Yin, Y.; Feng, X.; Nan, H.; Lin, J.; Ding, X.; Duan, W. Effects of Hot Isostatic Pressing and Heat Treatment on the Microstructure and Mechanical Properties of Cast TiAl Alloy. *Metals* **2021**, *11*, 1156. https://doi.org/10.3390/met11081156.
10. Sizova, I.; Sviridov, A.; Bambach, M.; Eisentraut, M.; Hemes, S.; Hecht, U.; Marquardt, A.; Leyens, C. A study on hot-working as alternative post-processing method for titanium aluminides built by laser powder bed fusion and electron beam melting. *J. Mater. Process. Technol.* **2021**, *291*, 117024. https://doi.org/10.1016/j.jmatprotec.2020.117024.
11. Polozov, I.; Kantyukov, A.; Goncharov, I.; Razumov, N.; Silin, A.; Popovich, V.; Zhu, J.-N.; Popovich, A. Additive Manufacturing of Ti-48Al-2Cr-2Nb Alloy Using Gas Atomized and Mechanically Alloyed Plasma Spheroidized Powders. *Materials* **2020**, *13*, 3952. https://doi.org/10.3390/ma13183952.
12. Biamino, S.; Penna, A.; Ackelid, U.; Sabbadini, S.; Tassa, O.; Fino, P.; Pavese, M.; Gennaro, P.; Badini, C. Electron beam melting of Ti-48Al-2Cr-2Nb alloy: Microstructure and mechanical properties investigation. *Intermetallics* **2011**, *19*, 776–781. https://doi.org/10.1016/j.intermet.2010.11.017.
13. Chowdhury, M.A.K.; Ullah, A.S.; Teti, R. Optimizing 3D Printed Metallic Object's Postprocessing: A Case of Gamma-TiAl Alloys. *Materials* **2021**, *14*, 1246. https://doi.org/10.3390/ma14051246.
14. Anwar, S. Electron beam melting of γ-TiAl and minimization of its surface roughness and cutting forces in turning. In Proceedings of the International Conference on Industrial Engineering and Operations Management, Dubai, UAE, 10–12 March 2020.
15. Tebaldo, V.; Faga, M.G. Influence of the heat treatment on the microstructure and machinability of titanium aluminides produced by electron beam melting. *J. Mater. Process. Technol.* **2017**, *244*, 289–303. https://doi.org/10.1016/j.jmatprotec.2017.01.037.
16. Mathew, N.T.; Vijayaraghavan, L. Environmentally friendly drilling of intermetallic titanium aluminide at different aspect ratio. *J. Clean. Prod.* **2017**, *141*, 439–452. https://doi.org/10.1016/j.jclepro.2016.09.125.

17. Castellanos, S.; Alves, J.L. A Review of Milling of Gamma Titanium Aluminides. *U. Porto J. Eng.* **2018**, *3*, 1–9. https://doi.org/10.24840/2183-6493_003.002_0001.

18. Wang, Z.; Liu, Y. Study of surface integrity of milled gamma titanium aluminide. *J. Manuf. Process.* **2020**, *56*, 806–819. https://doi.org/10.1016/j.jmapro.2020.05.021.

19. Priarone, P.C.; Klocke, F.; Faga, M.G.; Lung, D.; Settineri, L. Tool life and surface integrity when turning titanium aluminides with PCD tools under conventional wet cutting and cryogenic cooling. *Int. J. Adv. Manuf. Technol.* **2016**, *85*, 807–816. https://doi.org/10.1007/s00170-015-7958-5.

20. García-Martínez, E.; Miguel, V.; Martínez-Martínez, A.; Coello, J.; Naranjo, J.A.; Manjabacas, M.C. Optimization of the Dry Turning Process of Ti48Al2Cr2Nb Aluminide Based on the Cutting Tool Configuration. *Materials* **2022**, *15*, 1472. https://doi.org/10.3390/ma15041472.

21. Beranoagirre, A.; López de Lacalle, L.N. Optimizing the Turning of Titanium Aluminide Alloys. *Adv. Mater. Res.* **2012**, *498*, 189–194. https://doi.org/10.4028/www.scientific.net/AMR.498.189.

22. YAO, C.; LIN, J.; WU, D.; REN, J. Surface integrity and fatigue behavior when turning γ-TiAl alloy with optimized PVD-coated carbide inserts. *Chin. J. Aeronaut.* **2018**, *31*, 826–836. https://doi.org/10.1016/j.cja.2017.06.002.

23. Kolahdouz, S.; Hadi, M.; Arezoo, B.; Zamani, S. Investigation of surface integrity in high speed milling of gamma titanium aluminide under dry and minimum quantity lubricant conditions. *Procedia CIRP* **2015**, *26*, 367–372. https://doi.org/10.1016/j.procir.2014.08.016.

24. Aspinwall, D.K.; Dewes, R.C.; Mantle, A.L. The Machining of γ-TiAI Intermetallic Alloys. *CIRP Ann.* **2005**, *54*, 99–104. https://doi.org/10.1016/S0007-8506(07)60059-6.

25. Liang, X.; Liu, Z.; Wang, B.; Hou, X. Modeling of plastic deformation induced by thermo-mechanical stresses considering tool flank wear in high-speed machining Ti-6Al-4V. *Int. J. Mech. Sci.* **2018**, *140*, 1–12. https://doi.org/10.1016/j.ijmecsci.2018.02.031.

26. Priarone, P.C.; Rizzuti, S.; Rotella, G.; Settineri, L. Tool wear and surface quality in milling of a gamma-TiAl intermetallic. *Int. J. Adv. Manuf. Technol.* **2012**, *61*, 25–33. https://doi.org/10.1007/s00170-011-3691-x.

27. García-Martínez, E.; Miguel, V.; Martínez-Martínez, A.; Manjabacas, M.C.; Coello, J. Sustainable Lubrication Methods for the Machining of Titanium Alloys: An Overview. *Materials* **2019**, *12*, 3852. https://doi.org/10.3390/ma12233852.

28. Said, Z.; Gupta, M.; Hegab, H.; Arora, N.; Khan, A.M.; Jamil, M.; Bellos, E. A comprehensive review on minimum quantity lubrication (MQL) in machining processes using nano-cutting fluids. *Int. J. Adv. Manuf. Technol.* **2019**, *105*, 2057–2086. https://doi.org/10.1007/s00170-019-04382-x.

29. Priarone, P.C.; Robiglio, M.; Settineri, L.; Tebaldo, V. Milling and Turning of Titanium Aluminides by Using Minimum Quantity Lubrication. *Procedia CIRP* **2014**, *24*, 62–67. https://doi.org/10.1016/j.procir.2014.07.147.

30. Klocke, F.; Settineri, L.; Lung, D.; Claudio Priarone, P.; Arft, M. High performance cutting of gamma titanium aluminides: Influence of lubricoolant strategy on tool wear and surface integrity. *Wear* **2013**, *302*, 1136–1144. https://doi.org/10.1016/j.wear.2012.12.035.

31. García-Martínez, E.; Miguel, V.; Martínez-Martínez, A. Economic analysis of eco-friendly lubrication strategies for the machining of Ti48Al2Cr2Nb aluminide. *J. Clean. Prod.* **2024**, *435*, 140541. https://doi.org/10.1016/j.jclepro.2023.140541.

32. García-Martínez, E.; Miguel, V.; Manjabacas, M.C.; Martínez-Martínez, A.; Naranjo, J.A. Low initial lubrication procedure in the machining of copper-nickel 70/30 ASTM B122 alloy. *J. Manuf. Process.* **2021**, *62*, 623–631. https://doi.org/10.1016/j.jmapro.2021.01.002.

33. García-Martínez, E.; Martínez-Martínez, A.; Manjabacas, M.C.; Miguel, V. Proposal of a combined experimental-simulation methodology for the evaluation of machining temperature in turning processes. *Meas. J. Int. Meas. Confed.* **2022**, *189*, 110632.

34. Priarone, P.C.; Robiglio, M.; Settineri, L.; Tebaldo, V. Effectiveness of Minimizing Cutting Fluid Use when Turning Difficult-to-cut Alloys. *Procedia CIRP* **2015**, *29*, 341–346. https://doi.org/10.1016/j.procir.2015.02.006.

35. Anwar, S.; Ahmed, N.; Pervaiz, S.; Ahmad, S.; Mohammad, A.; Saleh, M. On the turning of electron beam melted gamma-TiAl with coated and uncoated tools: A machinability analysis. *J. Mater. Process. Technol.* **2020**, *282*, 116664. https://doi.org/10.1016/j.jmatprotec.2020.116664.

36. Cheng, Y.; Yuan, Q.; Zhang, B.; Wang, Z. Study on turning force of γ-TiAl alloy. *Int. J. Adv. Manuf. Technol.* **2019**, *105*, 2393–2402. https://doi.org/10.1007/s00170-019-04356-z.

37. Klocke, F.; Lung, D.; Arft, M.; Priarone, P.C.; Settineri, L. On high-speed turning of a third-generation gamma titanium aluminide. *Int. J. Adv. Manuf. Technol.* **2013**, *65*, 155–163. https://doi.org/10.1007/s00170-012-4157-5.